Journal of Membrane Science Letters 2 (2022) 100029

Contents lists available at ScienceDirect

Journal of Membrane Science Letters

journal homepage: www.elsevier.com/locate/memlet

Engineering MOF surface defects in mixed matrix membranes: An effective strategy to enhance MOF/polymer adhesion and control interfacial gas transport

Dong Fan[a,1], Aydin Ozcan[a,b,1], Osama Shekhah[c,d], Rocio Semino[a], Mohamed Eddaoudi[c,d,*], Guillaume Maurin[a,*]

[a] ICGM, Univ. Montpellier, CNRS, ENSCM, Montpellier, France
[b] TÜBITAK Marmara Research Center, Materials Technologies, 41470, Gebze, Kocaeli, Turkey
[c] King Abdullah University of Science and Technology (KAUST), Division of Physical Science and Engineering (PSE), Advanced Membrane and Porous Materials Center, Thuwal, 23955-6900, Saudi Arabia
[d] KAUST, Division of Physical Science and Engineering, Advanced Membrane and Porous Materials Center, Functional Materials Design, Discovery and Development (FMD^3), Thuwal, 23955-6900, Saudi Arabia

ARTICLE INFO

Keywords:
Metal–Organic Frameworks
Mixed Matrix Membranes
MOF surface defects
MOF/polymer adhesion
Gas transport
Molecular simulations

ABSTRACT

MOF/polymer adhesion in Mixed Matrix Membranes (MMMs) has been mainly enhanced so far via MOF and/or polymer functionalization to strengthen the interactions between the two components. This strategy, albeit effective, is generally accompanied by a drop in the permeability and/or selectivity performance of the MMMs. In this contribution, engineering structure defects at the MOF surfaces is proposed as an effective route to create pockets that immobilize part of the polymer chain, which is of crucial importance both to avoid plasticization issues and to enhance the MOF/polymer affinity while overcoming the adhesion/performance trade-off in MMMs. This engineered interfacial interlocking structure also serves as a bridge to accelerate the gas transport from the polymeric region towards the MOF pore entrance. This concept is showcased with a model MMM made of the prototypical UiO-66 MOF and the glassy Polymer of Intrinsic Microporosity-1 (PIM-1) and tested using CO_2, CH_4 and, N_2 as guest species. Our computational findings reveal that a defective UiO-66 MOF surface improves the MOF/PIM-1 adhesion and contributes to accelerate the interfacial gas transport of the slender molecules CO_2 and N_2 and in a lesser extent of the spherical molecule CH_4. This translates into a selective enhancement of the CO_2 transport once combined with CH_4 which paves the ways toward promising perspective for pre-combustion CO_2 capture.

Traditional separation and purification technologies, such as distillation, absorption, and extraction are extremely energy intensive. Thus, developing more cost-effective and sustainable separation techniques is a must to build a greener future (Sholl and Lively, 2016, Liu et al., 2018). Membrane-based separation offers a promising effective and economical solutions to a wide range of separations in both liquid and gas phases, owing to its low energy requirement and operational simplicity (Galizia et al., 2017, Koros and Zhang, 2017). Polymeric membranes have been widely considered both by academia (Merrick, Sujanani, and Freeman, 2020) and industry (PW, 2012) to tackle a myriad of challenging gas separations (Jimenez-Solomon et al., 2016, Mizrahi Rodriguez et al., 2021, Mizrahi Rodriguez et al., 2021). However, this family of membranes displays a trade-off between gas permeability and selectivity, as demonstrated by Robeson with his upper-bound curves (Robeson, 2008, Park et al., 2017). A new class of hybrid membranes integrating selective filler materials into a polymeric matrix has been further proposed to address this drawback (Qian et al., 2020). These so-called Mixed Matrix Membranes (MMMs) gather the best of the two worlds, i.e., easy processability/high durability of polymers and excellent selectivity of fillers (Knebel et al., 2020, Ahmad et al., 2018), and nowadays, they are the object of intensive research for various gas separation applications (Ahmad et al., 2018, Tien-Binh, Rodrigue, and Kaliaguine, 2018, Kamble, Patel, and Murthy, 2021). A vast variety of filler materials has been envisaged, including carbon nanotubes (Nejad, Asghari, and Afsari, 2016), graphene and related 2D materials (Dai et al., 2016), zeolites (Pechar et al., 2006), and more recently, porous Covalent Organic Frameworks (COFs) and Metal-Organic Frameworks (MOFs) (Park et al., 2017, Venna et al., 2015, Lee et al., 2021).

* Corresponding authors.
E-mail addresses: mohamed.eddaoudi@kaust.edu.sa (M. Eddaoudi), guillaume.maurin1@umontpellier.fr (G. Maurin).
[1] These authors contributed equally to the work.

https://doi.org/10.1016/j.memlet.2022.100029
Received 27 May 2022; Received in revised form 17 June 2022; Accepted 28 June 2022

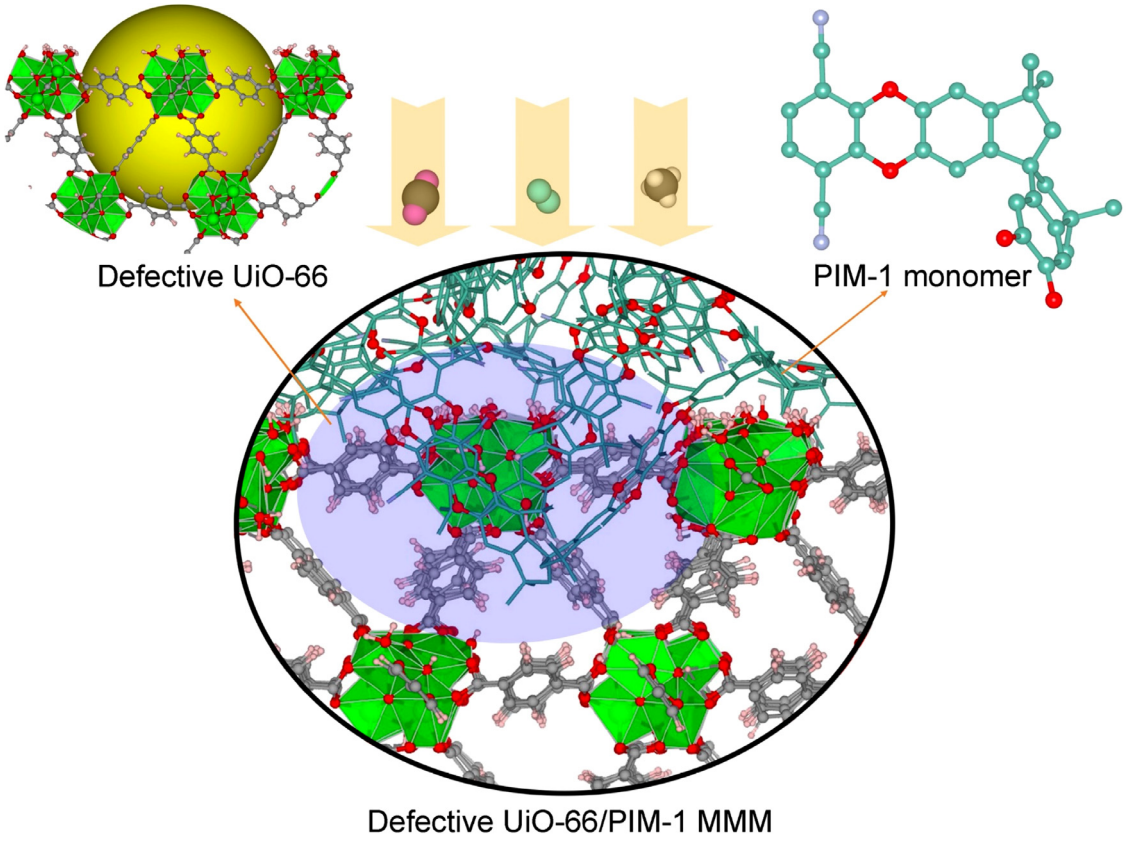

Scheme 1. MOF surface defects engineering as an alternative strategy to improve polymer plasticization, MOF/polymer adhesion, and interfacial gas transport in MMMs. The yellow ball represents the void that results from the missing cluster at the MOF surface in the UiO-66/PIM-1 MMM. Color code: carbon (PIM-1): cyan; oxygen: red; carbon (UiO-66): gray; nitrogen: blue; hydrogen: pink.

MMMs based on MOFs as fillers have been widely explored over the last few years, demonstrating attractive performance for a range of gas mixture separations related to CO_2 capture in post- or pre-combustion conditions, natural gas upgrading, and hydrocarbon recovery, among others challenging industrial processes (Bi et al., 2020, Zhang et al., 2016, Wang et al., 2021, Najari et al., 2021, Shan et al., 2018). In particular, researchers focused on the fabrication of MMMs combining highly permeable polymers such as the Polymer of Intrinsic Microporosity PIM-1 and selective MOFs (Knebel et al., 2020, Kalaj et al., 2020, Denny and Cohen, 2015, Troyano et al., 2018, Wang et al., 2018). One of the key challenges in the field is the fabrication of continuous and mechanically stable membranes, with high MOF loading and homogeneous dispersion of MOF nanoparticles into the polymer matrices that call for a good interfacial adhesion of the two components (Lin et al., 2018, Qian et al., 2019). A systematic computational exploration of the interface structures for a series of MOF/polymer composites has been achieved by our group via deploying an innovative modeling approach based on integrating quantum calculations and force-field molecular simulations (Tavares et al., 2019, Semino et al., 2018, Semino et al., 2016). This enabled us to unravel key features of both MOFs and polymers that control their adhesion (Tavares et al., 2019, Semino et al., 2018, Semino et al., 2016). The functionalization of MOFs and/or polymers has been widely envisaged to improve the adhesion of the two components in the MMMs (Ahmad et al., 2018, Venna et al., 2015, Tien-Binh et al., 2015, Carja et al., 2021, Ghalei et al., 2017, Sabetghadam et al., 2016, Rodenas et al., 2014, Wang et al., 2017, Ma et al., 2018, Amedi and Aghajani, 2017). However, with the exception of rare cases (Knebel et al., 2020, Tien-Binh et al., 2015), this strategy is accompanied by a loss of MMM performance in terms of either selectivity or permeability. For example, we evidenced that the functionalization of PIM-1 with amidoxime functions achieves an improvement of the adhesion with the UiO-66 MOF, however, at the expense of a substantial drop of gas permeability compared to the UiO-66/PIM-1 analogue (Carja et al., 2021). Polymer blending has also been proposed for improving the adhesion with the MOF, as for instance, with the addition of polybenzimidazole to the matrimid matrix to improve the compatibility of the interface formed with the hydrophobic MOFs ZIF-7 and ZIF-8, however, associated with a decrease of gas permeability (van Essen et al., 2021). Improvement of the adhesion was also recently achieved by polymer grafting on MOFs surfaces as show-cased with the UiO-66-NH_2 covalently grafted with poly(N-isopropylacrylamide) (Cseri et al., 2021, Benzaqui et al., 2019).

Herein structure defects that change the surface morphology are deliberately created at the MOF surface and their impact on the adhesion with the polymer and the interfacial gas transport in the so-formed MOF/polymer composite is computationally assessed (Scheme 1). The PIM-1/UiO-66 pair is considered as a show-case system, since (i) PIM-1 is a good candidate for MOF-based MMMs in account of its good permeability, intrinsic porosity while its rigid backbone generally leads to interfacial voids at the MOF surface in the MMM. (Tien-Binh, Rodrigue, and Kaliaguine, 2018, Carja et al., 2021, He et al., 2022) and (ii) UiO-66 is regarded as a prototypical defect-engineered MOF framework associated with a good chemical and mechanical stability (Tien-Binh, Rodrigue, and Kaliaguine, 2018, Qian et al., 2019, Carja et al., 2021, Lee et al., 2021, Wu, Yildirim, and Zhou, 2013, Liu et al., 2019). In previous work, the effect of chemical defects (removing the surface termination water-coordinated groups) in the MOF/polymer compatibility has been assessed (Semino et al., 2017). Recently, Yan *et al.* proposed a room-temperature elaboration of a pure defect-engineered UiO-66 membrane with enhanced CO_2/N_2 selectivity as compared to the

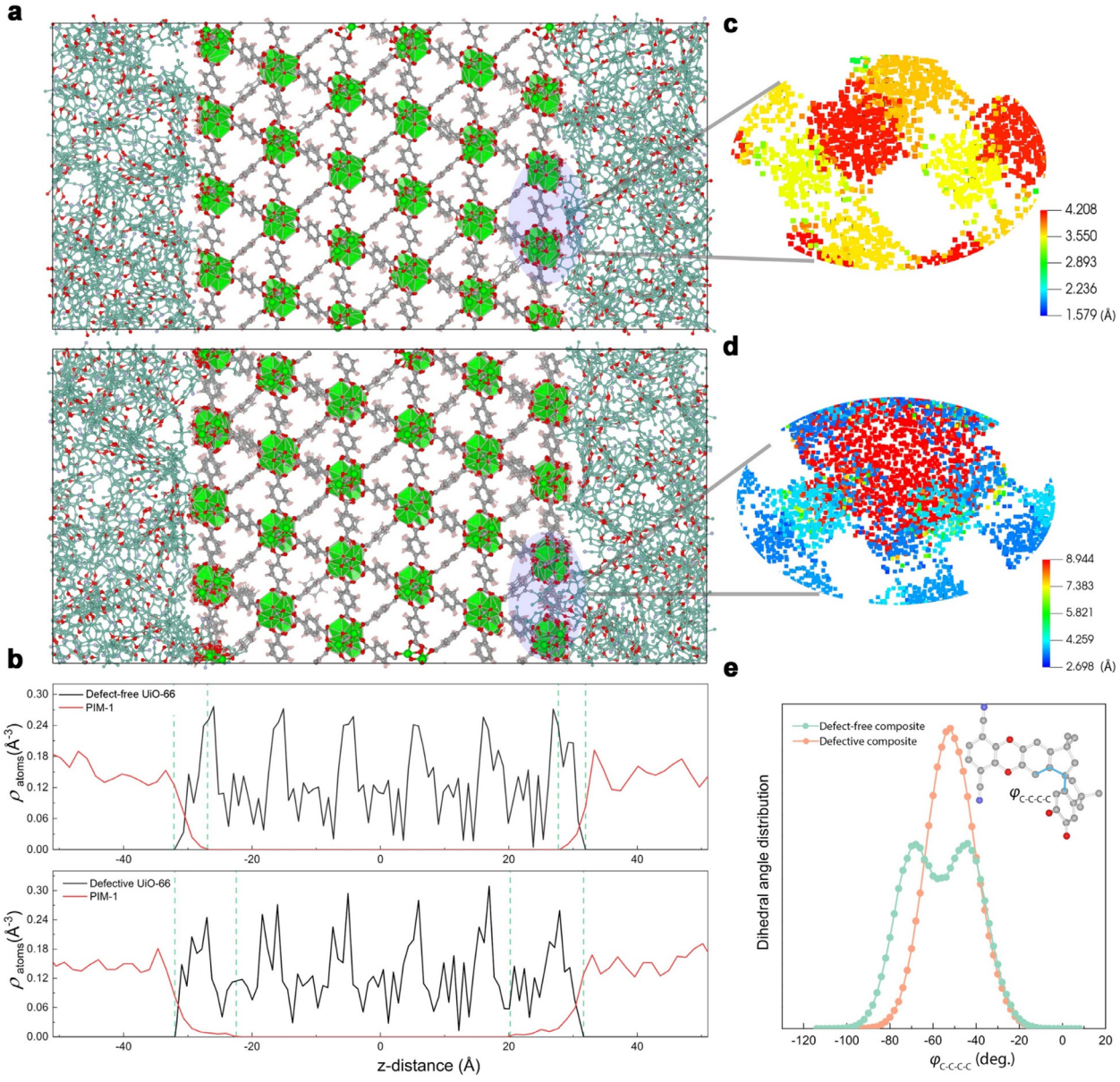

Fig. 1. (a) In silico constructed structures of the defect-free UiO-66/PIM-1 (upper) and defective UiO-66/PIM-1 (lower) composites, respectively. Color code: carbon (PIM-1): cyan; oxygen: red; carbon (UiO-66): gray; nitrogen: blue; hydrogen: pink. (b) Atomic density of PIM-1 (red) and both defect-free and defective UiO-66(Zr) (black) in the direction perpendicular to the surface slab for both composites. The center position of the MOF surface model was defined as zero. Pore size distribution of a zoom-in of the interfacial region for (c) defect-free UiO-66/PIM-1 and (d) defective UiO-66/PIM-1. (e) Dihedral angle $\varphi_{C-C-C-C}$ distribution of the PIM-1 section close to the UiO-66 surface calculated by E-MD simulations for both composites.

pristine UiO-66 membrane through attractive interactions between CO_2 and defect sites (Yan et al., 2022). The defects considered here extend to a larger scale (missing clusters), resulting in morphological changes in the surface, as opposed to a change in surface chemical functionality only. The computational approach we have previously developed (Semino et al., 2016) integrates density functional theory (DFT) calculations and flexible force field-based equilibrium molecular dynamics (E-MD) simulations to build atomistic models of the MOF/polymer interface. The MOF surface defects create an interfacial pocket that interlocks part of the polymer backbone and increases the MOF/polymer overlap, and hence the adhesion of the two components. Remarkably, concentration-gradient driven molecular dynamics (CGD-MD) calculations (Ozcan et al., 2017, Ozcan et al., 2020) revealed that this interfacial interlocking structure also accelerates the transport of CO_2, N_2 and in a lesser extent of CH_4 at the interfacial MOF/polymer region. This translates into a selective enhancement of the CO_2 transport once combined with CH_4 which is of interest for CO_2 capture under pre-combustion working conditions.

Atomistic models for defect-free and defective UiO-66/PIM-1 composites were first built. The models of the (101) defect-free UiO-66 surface slab and of the PIM-1 polymer united atom model were those from our previous work (Semino et al., 2018). The defective UiO-66 surface slab model was created by introducing 1 missing cluster at the outer surface, and the resulting under-coordinated atoms were saturated in a similar way that for the defect-free surface, i.e. Zr atoms are capped by OH^-, and the remaining H^+ that would result from the dissociative adsorption of water, form μ_3-OH groups with a framework oxygen atom at the MOF surface (see Figs. S1-S4). Force field parameters and MD simulation set-up information are provided in the ESI. Illustrative snapshots of the atomistic models for both defect-free and defective UiO-66/PIM-1 composites are shown in Fig. 1a. The UiO-66 slab models are located in the middle of the simulation box, surrounded by the PIM-1 polymer

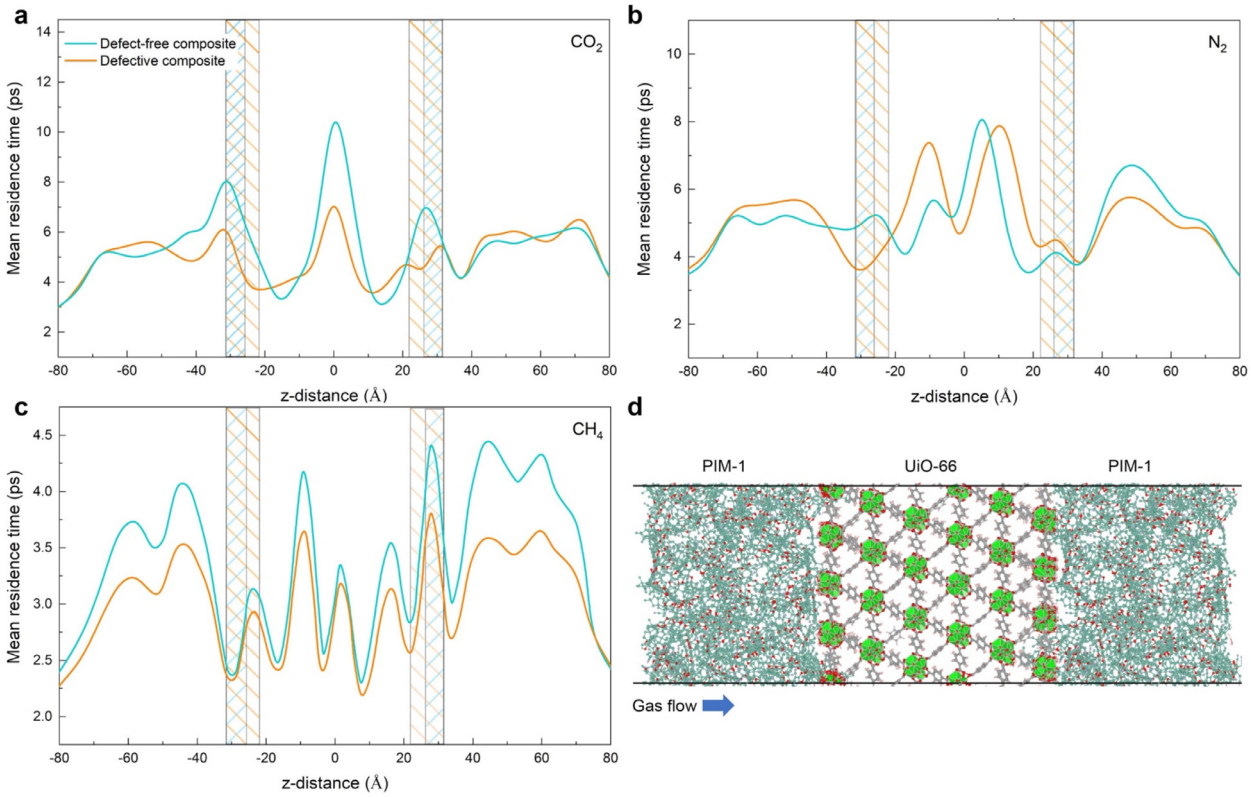

Fig. 2. CGD-MD simulated residence times at 298 K for CO_2 (a), N_2 (b), and CH_4 (c) along the z direction of both defect-free (blue colors) and defective UiO-66/PIM-1 (red colors) composite models. The center position of the MOF surface model is defined as zero. For clarity purposes, the interfacial MOF/polymer overlaps are marked in the shades of light green and orange for defect-free and defective UiO-66/PIM-1 composites, respectively. (d) Illustration of the typical UiO-66/PIM-1 composite model considered in the CGD-MD simulation. Color scheme: PIM-1, cyan wireframe; O, red; C (UiO-66), gray; H, white; Zr, green. The arrow on the bottom left margin points to the direction of the gas flux.

(Tavares et al., 2019, Semino et al., 2018, Semino et al., 2016). Fig. 1b reports the atomic density for both composites along the *z* direction normal to the MOF surface. Note that in both cases, the atomic density of PIM-1 oscillates around a mean-value far from the UiO-66s surface and it decays to zero at the close proximity to them. The MOF/polymer overlap length, which is defined as the distance between the *z* value for which the UiO-66 atomic density is zero and the *z* value for which the PIM-1 polymer atomic density vanishes (green dashed lines) is represented by green dashed lines in Fig. 1b. The overlap length is much larger in the case of the defective UiO-66 surface than for the defect-free-based composite (9.6 ± 0.3 Å vs. 5.2 ± 0.2 Å, respectively for values averaged over 5 different configurations for each case). This observation is in line with the presence of additional interfacial pockets created by the defective MOF surface with associated dimensions up to 9 Å (Fig. 1c and Fig. 1d), large enough to accommodate part of the polymer chain (Fig. 1b) thus enabling the polymer to better accomodate to the MOF surface. PIM-1 was found to occupy about 42% of the free volume of these interfacial pockets. While previous work (Semino et al., 2017) has demonstrated that defects that involve changes in the chemical functionality of the surface only have minor impact in the MOF/polymer compatibility, the structure defects that are studied in this work have a big impact in the compatibility, brought not by the site-site interactions but by a drastic change in the morphology of the MOF surface. Moreover, analysis of the polymer dihedral angle $\varphi_{C-C-C-C}$ distribution at the proximity of the MOF surface (see Fig. 1e) reveal that these interfacial pockets restrict the conformational dynamics of the PIM-1 backbone as indicated by a single $\varphi_{C-C-C-C}$ peak for the defective composite compared to two distinct and broader $\varphi_{C-C-C-C}$ distributions for the defect-free analogue. Overall these observations emphasize that the interfacial pockets contribute not only to enhancing the affinity between the MOF and the polymer but also to reducing the dynamics of the polymer, which may address plasticization issues often encountered in polymer-based membranes as well as to reduce the aging of PIM-1 as recently reported in the fabricated defective UiO-66/PIM MMM (Geng et al., 2022).

Therefore, engineering defects that modify the MOF surface morphology could be a complementary strategy to the standard functionalization approach largely explored so far from both MOF and polymer sides (Mizrahi Rodriguez et al., 2021, Mizrahi Rodriguez et al., 2021, Venna et al., 2015, Qian et al., 2019, Tien-Binh et al., 2015, Carja et al., 2021, Ghalei et al., 2017) to enhance MOF/polymer adhesion by tuning the interfacial pore geometry rather than modulating the interfacial interactions.

The so-depicted defective UiO-66/PIM-1 interfacial structure is expected to ensure a smoother transition for the guest molecules from the polymeric region to the MOF pore. CG-MD simulations were performed to explore the transport of CH_4, CO_2 and N_2 as single components throughout both defect-free and defective UiO-66/PIM-1 composites. These non-equilibrium MD simulations performed at 298 K using the GROMACS-2019.4 package patched with a modified PLUMED-2 enhanced sampling plug-in, considered larger and unwrapped composite models as illustrated in Fig. S6. A concentration gradient between the inlet (feed) and the outlet (permeate) sides of the composite was created by arbitrary fixing inlet and outlet pressures to 2 bar and vacuum, respectively, and 100 ns CGD-MD simulations were considered for each composite/gas pair after a 20 ns equilibration. All details and parameters of the CGD-MD calculations are provided in the ESI.

Fig. 2 reports the calculated residence times (τ) for the 3 gases along the z direction of defect-free and defective UiO-66/PIM-1 composites. Interestingly, the residence times at the MOF/polymer interface are shorter for all gases in the defective UiO-66/PIM-1 composite. Typi-

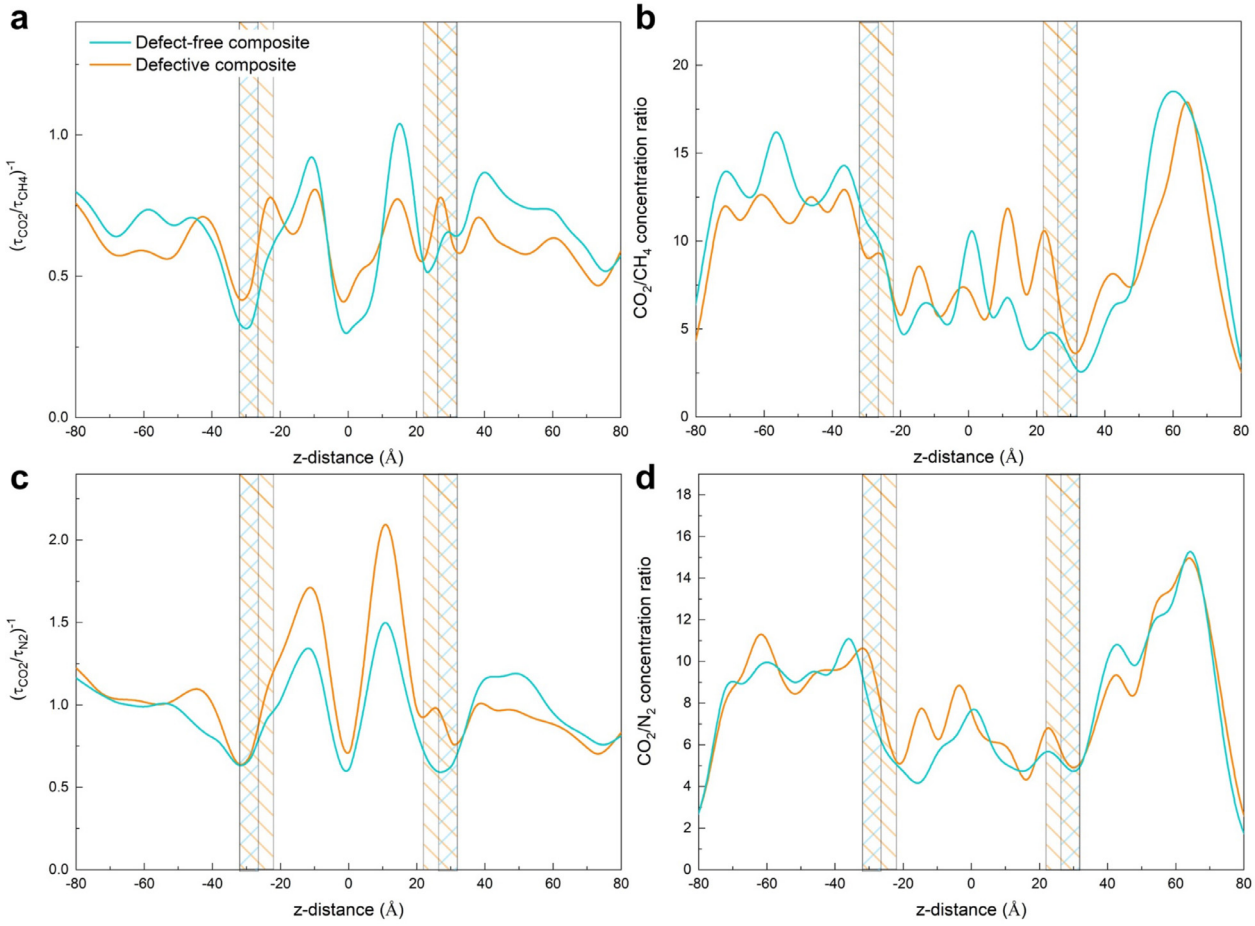

Fig. 3. (a, c) 1/residence time ($1/\tau$) and (b, d) concentration ratios plotted along the z direction of both defect-free and defective UiO-66/PIM-1 composite models: CO_2/CH_4 (top) and CO_2/N_2 (bottom) pairs. The MOF surface model is centered in zero, and the interfacial overlaps of MOF/Polymer are marked in the shades of light green and orange for defect-free and defective UiO-66/PIM-1 composites, as in Fig. 2.

cally, τ shows a maximum at the MOF/polymer interface for CO_2 that shifts from 8 ps to 6 ps when introducing defects at the MOF surface (Fig. 2a). This observation confirms that the interfacial pockets present in the defective composite not only do ensure better adhesion of the two components but also favor a faster transfer of the molecules from the polymer to the MOF pore entrance. Note from Fig. 2b and Fig. 2c that the decrease in the residence time at the MOF/polymer interface is less pronounced for N_2 and even less for CH_4 following the sequence of their kinetic diameters (CO_2<N_2<CH_4) and their bulkiness from slender (CO_2/N_2) to spherical (CH_4) shapes. This observation emphasizes the fact that the interfacial acceleration of the gas transport in the defective composite is mostly sterically-controlled since the gas molecules need to pass through the pockets that are already filled by a part of the PIM-1 chain.

As a further stage, the ratio of $1/\tau$ for both CO_2/CH_4 and CO_2/N_2 pairs was evaluated in both defect-free and defective UiO-66/PIM-1 composites from the τ values calculated for the single gases (Fig. 3). Since $1/\tau$ is related to the diffusivity of the molecules, Fig. 3a highlights that the MOF surface morphology changes enable a selective acceleration of the CO_2 transport over CH_4 at the UiO-66/PIM-1 interface while maintaining a similar CO_2/CH_4 concentration ratio (Fig. 3b) calculated from the single component steady state concentration profiles (Fig. S7). The scenario differs when one considers two molecules of similar shape, the slender CO_2 and N_2 molecules for which both $1/\tau$ (Fig. 3c) and concentration (Fig. 3d) ratios are only barely affected by the creation of MOF surface defects.

In summary, engineering structure defects at the UiO-66 surface is predicted to enhance the MOF/polymer adhesion in the corresponding defective UiO-66/PIM-1 composite by creating interfacial pockets that host part of the polymer backbone diminishing its conformational dynamics. The resulting interface with an optimal MOF/polymer overlap acts as an effective bridge to ensure a smooth transition for the gas molecules from the polymeric region to the MOF cage entrance. This translates into an acceleration of the interfacial molecular transport which is more pronounced for both slender-shaped molecules (CO_2, N_2) compared to the spherical-like CH_4 molecule. Notably, this phenomenon is expected to be associated with a selective enhancement of the CO_2 transport once combined with CH_4 which is of interest in the perspective of a pre-combustion CO_2 capture scenario. Beyond delivering an unprecedented understanding of the role of MOF surface morphology changing defects on the structure of the MOF/polymer interface and its guest dynamics, this computational work is expected to guide the development of more easily processable and highly selective MOF-based MMMs by deliberately introducing well-controlled morphology changes of the MOF surface.

Funding

The research reported in this publication was supported by King Abdullah University of Science and Technology (KAUST) (CCF 1972 project). The computational work was performed using HPC resources from GENCI-CINES (Grant A0120907613).

Conflicts of interest

The authors declare no conflict of interest.

Acknowledgements

The research reported in this publication was supported by King Abdullah University of Science and Technology (KAUST) (CCF 1972 project). The computational work was performed using HPC resources from GENCI-CINES (Grant A0120907613).

Supplementary materials

Supplementary material associated with this article can be found, in the online version, at doi:10.1016/j.memlet.2022.100029.

References

Ahmad, M.Z., Navarro, M., Lhotka, M., Zornoza, B., Téllez, C., de Vos, W.M., Benes, N.E., Konnertz, N.M., Visser, T., Semino, R., Maurin, G., Fila, V., Coronas, J., 2018. Enhanced gas separation performance of 6FDA-DAM based mixed matrix membranes by incorporating MOF UiO-66 and its derivatives. J. Membr. Sci. 558, 64–77. doi:10.1016/j.memsci.2018.04.040.

Amedi, H.R., Aghajani, M., 2017. Aminosilane-functionalized ZIF-8/PEBA mixed matrix membrane for gas separation application. Microporous Mesoporous Mater. 247, 124–135. doi:10.1016/j.micromeso.2017.04.001.

Benzaqui, M., Semino, R., Carn, F., Tavares, S.R., Menguy, N., Giménez-Marqués, M., Bellido, E., Horcajada, P., Berthelot, T., Kuzminova, A.I., Dmitrenko, M.E., Penkova, A.V., Roizard, D., Serre, C., Maurin, G., Steunou, N., 2019. Covalent and selective grafting of polyethylene glycol brushes at the surface of ZIF-8 for the processing of membranes for pervaporation. ACS Sustain. Chem. Eng. 7 (7), 6629–6639. doi:10.1021/acssuschemeng.8b05587.

Bi, X., Zhang, Y., Zhang, F., Zhang, S., Wang, Z., Jin, J., 2020. MOF nanosheet-based mixed matrix membranes with Metal-organic coordination interfacial interaction for gas separation. ACS Appl. Mater. Interfaces 12 (43), 49101–49110. doi:10.1021/acsami.0c14639.

Carja, I.-D., Tavares, S.R., Shekhah, O., Ozcan, A., Semino, R., Kale, V.S., Eddaoudi, M., Maurin, G., 2021. Insights into the enhancement of mof/polymer adhesion in mixed-matrix membranes *via* polymer functionalization. ACS Appl. Mater. Interfaces 13 (24), 29041–29047. doi:10.1021/acsami.1c03859.

Cseri, L., Hardian, R., Anan, S., Vovusha, H., Schwingenschlögl, U., Budd, P.M., Sada, K., Kokado, K., Szekely, G, 2021. Bridging the interfacial gap in mixed-matrix membranes by nature-inspired design: precise molecular sieving with polymer-grafted metal-organic frameworks. J. Mater. Chem. A 9 (42), 23793–23801. doi:10.1039/D1TA06205K.

Dai, Y., Ruan, X., Yan, Z., Yang, K., Yu, M., Li, H., Zhao, W., He, G., 2016. Imidazole functionalized graphene Oxide/PEBAX Mixed Matrix Membranes for Efficient CO2 Capture. Sep. Purif. Technol. 166, 171–180. doi:10.1016/j.seppur.2016.04.038.

Denny, M.S., Cohen, S.M., 2015. In Situ modification of metal-organic frameworks in mixed-matrix membranes. Angew. Chem. Int. Ed. 54 (31), 9029–9032. doi:10.1002/anie.201504077.

Galizia, M., Chi, W.S., Smith, Z.P., Merkel, T.C., Baker, R.W., Freeman, B.D., 2017. 50th Anniversary perspective: polymers and mixed matrix membranes for gas and vapor separation: a review and prospective opportunities. Macromolecules 50 (20), 7809–7843. doi:10.1021/acs.macromol.7b01718.

Geng, C., Sun, Y., Zhang, Z., Qiao, Z., Zhong, C, 2022. Mitigated aging in a defective metal-organic framework pillared polymer of an intrinsic porosity hybrid membrane for efficient gas separation. ACS Sustain. Chem. Eng. 10 (11), 3643–3650. doi:10.1021/acssuschemeng.1c08485.

Ghalei, B., Sakurai, K., Kinoshita, Y., Wakimoto, K., Isfahani, A.P., Song, Q., Doitomi, K., Furukawa, S., Hirao, H., Kusuda, H., Kitagawa, S., Sivaniah, E., 2017. Enhanced selectivity in mixed matrix membranes for CO2 capture through efficient dispersion of amine-functionalized MOF nanoparticles. Nat. Energy 2 (7), 17086. doi:10.1038/nenergy.2017.86.

He, S., Zhu, B., Li, S., Zhang, Y., Jiang, X., Hon Lau, C., Shao, L., 2022. Recent progress in PIM-1 based membranes for sustainable CO2 separations: polymer structure manipulation and mixed matrix membrane design. Sep. Purif. Technol. 284, 120277. doi:10.1016/j.seppur.2021.120277.

Jimenez-Solomon, M.F., Song, Q., Jelfs, K.E., Munoz-Ibanez, M., Livingston, A.G., 2016. Polymer Nanofilms with Enhanced Microporosity by Interfacial Polymerization. Nat. Mater. 15 (7), 760–767. doi:10.1038/nmat4638.

Kalaj, M., Bentz, K.C., Ayala, S., Palomba, J.M., Barcus, K.S., Katayama, Y., Cohen, S.M., 2020. MOF-polymer hybrid materials: from simple composites to tailored architectures. Chem. Rev. 120 (16), 8267–8302. doi:10.1021/acs.chemrev.9b00575.

Kamble, A.R., Patel, C.M., Murthy, Z.V.P., 2021. A review on the recent advances in mixed matrix membranes for gas separation processes. Renew. Sustain. Energy Rev. 145, 111062. doi:10.1016/j.rser.2021.111062.

Knebel, A., Bavykina, A., Datta, S.J., Sundermann, L., Garzon-Tovar, L., Lebedev, Y., Durini, S., Ahmad, R., Kozlov, S.M., Shterk, G., Karunakaran, M., Carja, I.D., Simic, D., Weilert, I., Klüppel, M., Giese, U., Cavallo, L., Rueping, M., Eddaoudi, M., Caro, J., Gascon, J, 2020. Solution processable metal-organic frameworks for mixed matrix membranes using porous liquids. Nat. Mater. 19 (12), 1346–1353. doi:10.1038/s41563-020-0764-y.

Koros, W.J., Zhang, C., 2017. Materials for next-generation molecularly selective synthetic membranes. Nature Mater 16 (3), 289–297. doi:10.1038/nmat4805.

Lee, T.H., Jung, J.G., Kim, Y.J., Roh, J.S., Yoon, H.W., Ghanem, B.S., Kim, H.W., Cho, Y.H., Pinnau, I., Park, H.B., 2021. Defect engineering in metal-organic frameworks towards advanced mixed matrix membranes for efficient propylene/propane separation. Angew. Chem. 133 (23), 13191–13198. doi:10.1002/ange.202100841.

Lee, T.H., Ozcan, A., Park, I., Fan, D., Jang, J.K., Mileo, P.G.M., Yoo, S.Y., Roh, J.S., Kang, J.H., Lee, B.K., Cho, Y.H., Semino, R., Kim, H.W., Maurin, G., Park, H.B., 2021. Disclosing the role of defect-engineered metal-organic frameworks in mixed matrix membranes for efficient CO_2 separation: a joint experimental-computational exploration. Adv. Funct. Mater. 31 (38), 2103973. doi:10.1002/adfm.202103973.

Lin, R., Villacorta Hernandez, B., Ge, L., Zhu, Z, 2018. Metal organic framework based mixed matrix membranes: an overview on filler/polymer interfaces. J. Mater. Chem. A 6 (2), 293–312. doi:10.1039/C7TA07294E.

Liu, G., Chernikova, V., Liu, Y., Zhang, K., Belmabkhout, Y., Shekhah, O., Zhang, C., Yi, S., Eddaoudi, M., Koros, W.J., 2018. Mixed matrix formulations with MOF molecular sieving for key energy-intensive separations. Nature Mater 17 (3), 283–289. doi:10.1038/s41563-017-0013-1.

Liu, L., Chen, Z., Wang, J., Zhang, D., Zhu, Y., Ling, S., Huang, K.-W., Belmabkhout, Y., Adil, K., Zhang, Y., Slater, B., Eddaoudi, M., Han, Y, 2019. Imaging defects and their evolution in a metal-organic framework at sub-unit-cell resolution. Nat. Chem. 11 (7), 622–628. doi:10.1038/s41557-019-0263-4.

Ma, X., Swaidan, R.J., Wang, Y., Hsiung, C., Han, Y., Pinnau, I., 2018. Highly compatible hydroxyl-functionalized microporous Polyimide-ZIF-8 mixed matrix membranes for energy efficient propylene/propane separation. ACS Appl. Nano Mater 1 (7), 3541–3547. doi:10.1021/acsanm.8b00682.

Merrick, M.M., Sujanani, R., Freeman, B.D., 2020. Glassy polymers: historical findings, membrane applications, and unresolved questions regarding physical aging. Polymer 211, 123176. doi:10.1016/j.polymer.2020.123176.

Mizrahi Rodriguez, K., Benedetti, F.M., Roy, N., Wu, A.X., Smith, Z.P, 2021. Sorption-enhanced mixed-gas transport in amine functionalized polymers of intrinsic microporosity (PIMs). J. Mater. Chem. A 9 (41), 23631–23642. doi:10.1039/D1TA06530K.

Mizrahi Rodriguez, K., Lin, S., Wu, A.X., Han, G., Teesdale, J.J., Doherty, C.M., Smith, Z.P, 2021. Leveraging free volume manipulation to improve the membrane separation performance of amine-functionalized PIM-1. Angew. Chem. Int. Ed Engl. 60 (12), 6593–6599. doi:10.1002/anie.202012441.

Najari, S., Saeidi, S., Gallucci, F., Drioli, E., 2021. Mixed matrix membranes for hydrocarbons separation and recovery: a critical review. Rev. Chem. Eng. 37 (3), 363–406. doi:10.1515/revce-2018-0091.

Nejad, M.N., Asghari, M., Afsari, M., 2016. Investigation of carbon nanotubes in mixed matrix membranes for gas separation: a review. ChemBioEng Rev. 3 (6), 276–298. doi:10.1002/cben.201600012.

Ozcan, A., Perego, C., Salvalaglio, M., Parrinello, M., Yazaydin, O., 2017. Concentration gradient driven molecular dynamics: a new method for simulations of membrane permeation and separation. Chem. Sci. 8 (5), 3858–3865. doi:10.1039/C6SC04978H.

Ozcan, A., Semino, R., Maurin, G., Yazaydin, A.O., 2020. Modeling of gas transport through polymer/MOF interfaces: a microsecond-scale concentration gradient-driven molecular dynamics study. Chem. Mater. 32 (3), 1288–1296. doi:10.1021/acs.chemmater.9b04907.

Park, H.B., Kamcev, J., Robeson, L.M., Elimelech, M., Freeman, B.D., 2017. Maximizing the right stuff: the trade-off between membrane permeability and selectivity. Science 356 (6343), eaab0530. doi:10.1126/science.aab0530.

Pechar, T.W., Kim, S., Vaughan, B., Marand, E., Tsapatsis, M., Jeong, H.K., Cornelius, C.J., 2006. Fabrication and characterization of polyimide-Zeolite L mixed matrix membranes for gas separations. J. Membr. Sci. 277 (1), 195–202. doi:10.1016/j.memsci.2005.10.029.

PW, B., 2012. Membrane Technology and Applications. John Wiley & Sons.

Qian, Q., Asinger, P.A., Lee, M.J., Han, G., Mizrahi Rodriguez, K., Lin, S., Benedetti, F.M., Wu, A.X., Chi, W.S., Smith, Z.P., 2020. MOF-based membranes for gas separations. Chem. Rev. 120 (16), 8161–8266. doi:10.1021/acs.chemrev.0c00119.

Qian, Q., Wu, A.X., Chi, W.S., Asinger, P.A., Lin, S., Hypsher, A., Smith, Z.P., 2019. Mixed-matrix membranes formed from imide-functionalized UiO-66-NH_2 for improved interfacial compatibility. ACS Appl. Mater. Interfaces 11 (34), 31257–31269. doi:10.1021/acsami.9b07500.

Robeson, L.M., 2008. The Upper Bound Revisited. J. Membr. Sci. 320 (1-2), 390–400. doi:10.1016/j.memsci.2008.04.030.

Rodenas, T., van Dalen, M., García-Pérez, E., Serra-Crespo, P., Zornoza, B., Kapteijn, F., Gascon, J., 2014. Visualizing MOF mixed matrix membranes at the nanoscale: towards structure-performance relationships in CO_2 /CH_4 separation Over NH_2 -MIL-53(Al)@PI. Adv. Funct. Mater 24 (2), 249–256. doi:10.1002/adfm.201203462.

Sabetghadam, A., Seoane, B., Keskin, D., Duim, N., Rodenas, T., Shahid, S., Sorribas, S., Guillouzer, C.L., Clet, G., Tellez, C., Daturi, M., Coronas, J., Kapteijn, F., Gascon, J., 2016. Metal organic framework crystals in mixed-matrix membranes: impact of the filler morphology on the gas separation performance. Adv. Funct. Mater. 26 (18), 3154–3163. doi:10.1002/adfm.201505352.

Semino, R., Moreton, J.C., Ramsahye, N.A., Cohen, S.M., Maurin, G., 2018. Understanding the origins of metal-organic framework/polymer compatibility. Chem. Sci. 9 (2), 315–324. doi:10.1039/C7SC04152G.

Semino, R., Ramsahye, N.A., Ghoufi, A., Maurin, G., 2016. Microscopic model of the metal-organic framework/polymer interface: a first step toward understanding the compatibility in mixed matrix membranes. ACS Appl. Mater. Interfaces 8 (1), 809–819. doi:10.1021/acsami.5b10150.

Semino, R., Ramsahye, N.A., Ghoufi, A., Maurin, G., 2017. Role of MOF surface defects on the microscopic structure of MOF/Polymer interfaces: a computational

study of the ZIF-8/PIMs systems. Microporous Mesoporous Mater. 254, 184–191. doi:10.1016/j.micromeso.2017.02.031.

Shan, M., Seoane, B., Andres-Garcia, E., Kapteijn, F., Gascon, J., 2018. Mixed-matrix membranes containing an azine-linked covalent organic framework: influence of the polymeric matrix on post-combustion CO2-capture. J. Membr. Sci. 549, 377–384. doi:10.1016/j.memsci.2017.12.008.

Sholl, D.S., Lively, R.P., 2016. Seven chemical separations to change the world. Nature 532 (7600), 435–437. doi:10.1038/532435a.

Tavares, S.R., Ramsahye, N.A., Adil, K., Eddaoudi, M., Maurin, G., Semino, R., 2019. Computationally assisted assessment of the metal-organic framework/polymer compatibility in composites integrating a rigid polymer. Adv. Theory Simul. 2 (11), 1900116. doi:10.1002/adts.201900116.

Tien-Binh, N., Rodrigue, D., Kaliaguine, S., 2018. In-Situ cross interface linking of PIM-1 polymer and UiO-66-NH2 for outstanding gas separation and physical aging control. J. Membr. Sci. 548, 429–438. doi:10.1016/j.memsci.2017.11.054.

Tien-Binh, N., Vinh-Thang, H., Chen, X.Y., Rodrigue, D., Kaliaguine, S., 2015. Polymer functionalization to enhance interface quality of mixed matrix membranes for high CO_2/CH_4 gas separation. J. Mater. Chem. A 3 (29), 15202–15213. doi:10.1039/C5TA01597A.

Troyano, J., Carné-Sánchez, A., Pérez-Carvajal, J., León-Reina, L., Imaz, I., Cabeza, A., Maspoch, D., 2018. A self-folding polymer film based on swelling metal-organic frameworks. Angew. Chem. 130 (47), 15646–15650. doi:10.1002/ange.201808433.

van Essen, M., Thür, R., van den Akker, L., Houben, M., Vankelecom, I.F.J., Nijmeijer, K., Borneman, Z., 2021. Tailoring the separation performance of ZIF-based mixed matrix membranes by MOF-matrix interfacial compatibilization. J. Membr. Sci. 637, 119642. doi:10.1016/j.memsci.2021.119642.

Venna, S.R., Lartey, M., Li, T., Spore, A., Kumar, S., Nulwala, H.B., Luebke, D.R., Rosi, N.L., Albenze, E, 2015. Fabrication of MMMs with improved gas separation properties using externally-functionalized MOF particles. J. Mater. Chem. A 3 (9), 5014–5022. doi:10.1039/C4TA05225K.

Wang, H., He, S., Qin, X., Li, C., Li, T, 2018. Interfacial engineering in metal-organic framework-based mixed matrix membranes using covalently grafted polyimide brushes. J. Am. Chem. Soc. 140 (49), 17203–17210. doi:10.1021/jacs.8b10138.

Wang, Z., Ren, H., Zhang, S., Zhang, F., Jin, J., 2017. Polymers of intrinsic microporosity/metal-organic framework hybrid membranes with improved interfacial interaction for high-performance CO_2 separation. J. Mater. Chem. A 5 (22), 10968–10977. doi:10.1039/C7TA01773A.

Wang, Z., Tian, Y., Fang, W., Shrestha, B.B., Huang, M., Jin, J., 2021. Constructing strong interfacial interactions under mild conditions in MOF-incorporated mixed matrix membranes for gas separation. ACS Appl. Mater. Interfaces 13 (2), 3166–3174. doi:10.1021/acsami.0c19554.

Wu, H., Yildirim, T., Zhou, W., 2013. Exceptional mechanical stability of highly porous zirconium metal-organic framework UiO-66 and its important implications. J. Phys. Chem. Lett. 4 (6), 925–930. doi:10.1021/jz4002345.

Yan, J., Sun, Y., Ji, T., Zhang, C., Liu, L., Liu, Y., 2022. Room-temperature synthesis of defect-engineered zirconium-MOF membrane enabling superior CO2/N2 selectivity with Zirconium-Oxo cluster source. J. Membr. Sci. 653, 120496. doi:10.1016/j.memsci.2022.120496.

Zhang, Y., Feng, X., Yuan, S., Zhou, J., Wang, B., 2016. Challenges and recent advances in MOF-polymer composite membranes for gas separation. Inorg. Chem. Front. 3 (7), 896–909. doi:10.1039/C6QI00042H.